

Mining the Biosynthetic Landscape of Lactic Acid Bacteria Unearths a New Family of RiPPs Assembled by a Novel Type of ThiF-like Adenylyltransferases

Mengjiao Wang,[#] Mengyue Wu,[#] Meng Han, Xiaogang Niu, Aili Fan,^{*} Shaozhou Zhu,^{*} and Yigang Tong^{*}



Cite This: *ACS Omega* 2024, 9, 30891–30903



Read Online

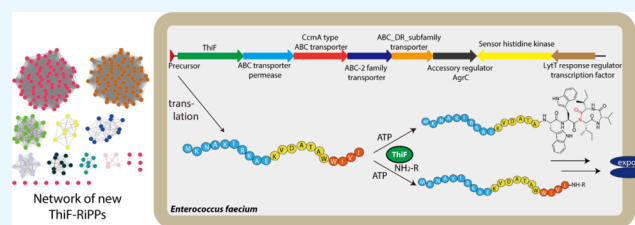
ACCESS |

Metrics & More

Article Recommendations

Supporting Information

ABSTRACT: Ribosomally synthesized and post-translationally modified peptides (RiPPs) are chemically diverse natural products of ribosomal origin. These peptides, which frequently act as signals or antimicrobials, are biosynthesized by conserved enzymatic machinery, making genome mining a powerful strategy for unearthing previously uncharacterized members of their class. Herein, we investigate the untapped biosynthetic potential of Lactobacillales (i.e., lactic acid bacteria), an order of Gram-positive bacteria closely associated with human life, including pathogenic species and industrially relevant fermenters of dairy products. Through genome mining methods, we systematically explored the distribution and diversity of ThiF-like adenylyltransferase-utilizing RiPP systems in lactic acid bacteria and identified a number of unprecedented biosynthetic gene clusters. In one of these clusters, we found a previously undescribed group of macrocyclic imide biosynthetic pathways containing multiple transporters that may be involved in a potential quorum sensing (QS) system. Through *in vitro* assays, we determined that one such adenylyltransferase specifically catalyzes the intracyclization of its precursor peptide through macrocyclic imide formation. Incubating the enzyme with various primary amines revealed that it could effectively amidate the C-terminus of the precursor peptide. This new transformation adds to the growing list of Nature's peptide macrocyclization strategies and expands the impressive catalytic repertoire of the adenylyltransferase family. The diverse RiPP systems identified herein represent a vast, unexploited landscape for the discovery of a novel class of natural products and QS systems.



INTRODUCTION

Ribosomally synthesized and post-translationally modified peptides (RiPPs) are a growing family of natural products that exhibit remarkable chemical diversity despite their ribosomal origin. On account of their complex structures, these peptides carry out an array of medically relevant functions, serving as antibiotics, anticancer agents, cofactors, signals, and toxins.^{1,2}

Typically, RiPPs are biosynthesized as precursor peptides consisting of two parts: an N-terminal leader sequence, which is bound and recognized by processing enzymes, and a C-terminal core sequence, which is matured by that machinery.³ Often, the leader sequence is proteolytically cleaved during processing, freeing the core scaffold for further embellishment by option tailoring enzymes prior to transporter-mediated export from the cell. Much of the chemical (and thus functional) diversity of RiPPs hinges on cyclization reactions that substantially alter the three-dimensional shape of the peptide, resulting in, e.g., proteolytic stability and/or affinity for specific molecular targets (Figure 1).⁴

ATP/Mg²⁺-dependent activation of the precursor peptide with phosphate or AMP is a common strategy for forming cyclic moieties during RiPP biosynthesis.⁴ For example, it is employed to generate the heterocycles of thiazole/oxazole-modified

microcins (LAPs; e.g., microcin B17),^{5,6} the cyclic thioethers of lanthipeptides (e.g., lacticin 481),⁷ and the macrolactams of microviridins and lasso peptides (Figure 1A).^{8–10}

A distinctive set of enzymatic machinery has evolved to install the characteristic cyclic features in each of these RiPP subfamilies. For instance, the cyclodehydration reactions in LAP biosynthesis require a protein homologous to the adenylyltransferases ThiF, MoeB, and ubiquitin-activating enzyme E1 that bind and adenylate their substrates during thiamine or molybdopterin biosynthesis and protein ubiquitination, respectively.^{11–13} Unlike ThiF, MoeB, and E1, however, the ATP-binding site is perturbed, and no ATP consumption has been demonstrated for the homologues involved in LAP assembly (e.g., McbB for microcin B17); instead, the latter appears to bind the peptide substrate, assisted by an N-terminal

Received: April 19, 2024

Revised: June 22, 2024

Accepted: June 25, 2024

Published: July 3, 2024



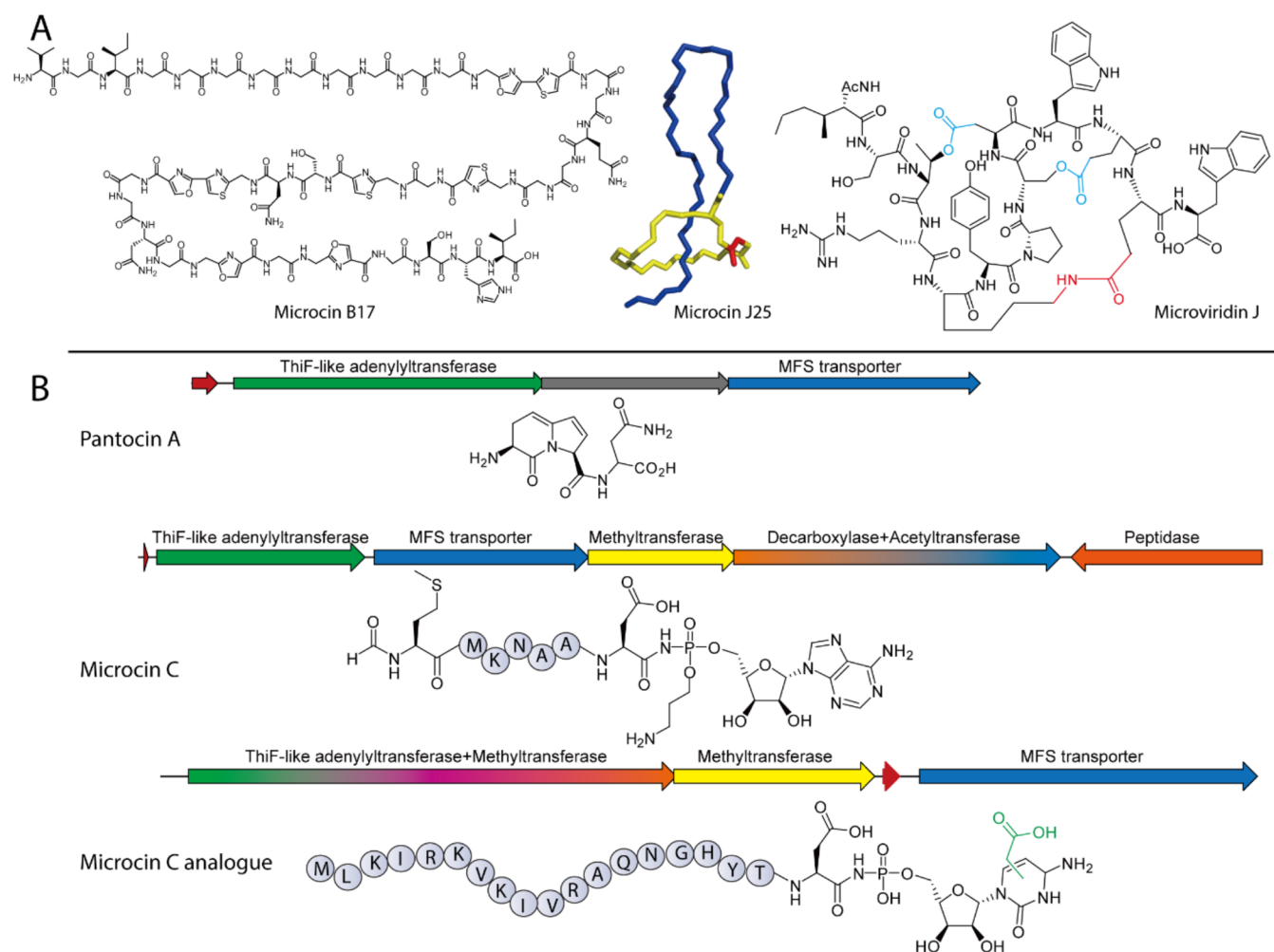


Figure 1. (A) Representative structures of known cyclic peptides with isopeptide bonds. (B) Known RiPP biosynthetic gene clusters containing ThiF enzymes, including pantocin A, microcin C, and microcin C analogue.

RiPP precursor peptide recognition element (RRE),¹⁴ and deliver it to an ATP-dependent YcaO-like enzyme for cyclization (e.g., McbD for microcin B17).^{15–18}

Conversely, adenylyltransferases from other RiPP systems, like those of pantocin A and microcin C, function more like ThiF, MoeB, and E1 by directly activating the C-termini of their substrates with AMP, again with support from RREs (we refer to these homologues hereafter as ThiF-like adenylyltransferases, or TLATs).^{11,19} Past research correlated the RiPP gene cluster *paaPABC* from *Pantoea agglomerans* with the biosynthesis of pantocin A, a natural product that exerts its antibiotic activity through the inhibition of L-histidinol phosphate aminotransferase (Figure 1B).^{20,21} More recent *in vitro* investigations revealed that TLAT PaaA promotes ATP-dependent intramolecular cyclization through two dehydrations and one decarboxylation of the Glu pair in the middle of precursor peptide PaaP, leading to the formation of the bicyclic core of pantocin A.¹⁹ α -Ketoglutarate-dependent iron oxidase PaaB, an unidentified peptidase, and ATP-binding cassette (ABC) transporter PaaC then catalyze dehydrogenation, proteolysis, and efflux, respectively.^{19,20}

Microcin C, on the other hand, is an aspartyl-tRNA synthetase-targeting antibiotic produced by a plasmid-born *mccABCDEF* gene cluster in *Escherichia coli* (Figure 1B).^{22,23} This N-formylated heptapeptide (MRTGNAD) is linked at its

C-terminus to AMP via an N–P bond, installed by TLAT MccB in two ATP-dependent reactions: intramolecular cyclization between Asn and the C-terminus to form a peptidyl-succinimide intermediate, followed by adenylation of the succinimidyl N atom and hydrolytic opening of the succinimide ring.²⁴ Finally, S-adenosylmethionine (SAM)-dependent methyltransferase and pyridoxyl 5'-phosphate (PLP)-dependent decarboxylase homologues MccD and MccE attach propylamine to the phosphate group, major facilitator superfamily (MFS) transporter MccC exports the compound from the cell, and serine protease MccF provides immunity.^{22,23,25–27}

Recently, a microcin C analogue consisting of a 19-residue peptidyl region and a carboxymethyl-modified cytidine moiety in place of the C-terminal adenosine was discovered from *Bacillus amyloliquefaciens* (Figure 1B).²⁸ The MccB homologue from this pathway was shown to accept all four NTPs *in vitro*, albeit with a striking preference for CTP, in agreement with the peptidyl-cytidylate isolated from bacilli. Furthermore, a C-terminal extension to MccB, identified as a SAM-dependent methyltransferase homologue, was confirmed to install the carboxymethyl group in conjunction with carboxy-SAM synthetase homologue MccS. As in the *E. coli* gene cluster, a gene coding for an MFS transporter likely responsible for the export of the antibiotic was observed.

Severinov and colleagues previously identified and/or functionally validated additional homologues of PaaA, MccB, and associated precursor peptides, which are encoded not only in Gram-negative bacteria but also in *Bacillota* and *Cyanobacteria*.^{29,30} This finding suggests that many more TLATs, and thus pantocin A- and microcin C-like RiPPs, remain to be discovered. More recently, Seyedsayamdost and colleagues have shown that ThiF-like adenylyltransferase/cyclase is also involved in the biosynthesis of RiPPs tailored by radical S-adenosylmethionine (RaS) enzymes in streptococci. This enzyme can generate a C-terminal Glu-to-Cys thiolactone macrocycle, further demonstrating the versatility of these enzymes.³¹

Given the few but diverse TLAT-RiPP systems that have been characterized, we decided to seek further examples. We began by mining for homologues of MccB in the genomes of lactic acid bacteria. On account of their relatively compact genomes, this order of Gram-positive bacteria, consisting of human commensals and opportunistic pathogens as well as food industry mainstays,^{32–34} has been underexploited for natural product discovery.^{35,36} Our efforts uncovered an extensive collection of BGCs that, based on their unique architectures, appear to encode RiPPs decorated with previously undescribed post-translational modifications. A second stage of mining performed without limiting genomes to lactic acid bacteria revealed that RiPP-associated TLATs are employed liberally across the bacterial kingdom. We selected one TLAT identified from *Enterococcus faecalis* FDAARGOS_397, EnfB, for further characterization, which led to the discovery of enterofaecin, a new type of RiPPs containing a macrocyclic imide distinct from succinimide. We also found that, in the presence of EnfB, the enterofaecin precursor undergoes C-terminal amidation by various primary amines. The association of several ATP-binding cassette (ABC) transporters and a novel QS system indicated that this biosynthetic logic might play important physiological roles, such as virulence or interspecies communication. Our studies open an avenue to a vast network of RiPPs with unprecedented catalytic inventory and yet-to-be-explored biological functions.

MATERIALS AND METHODS

Bioinformatics Studies. Genome mining studies were performed using the web-based bioinformatics tool PSI-BLAST, with MccB^{Eco} (AAY68495.1) as the query sequence.³⁷ Algorithm parameters were set as follows: maximum target sequences, 1000; expected threshold, 10; and matrix, BLOSUM62. The organism was limited to either *Streptococcus* (taxid: 1301) or *Enterococcus* (taxid: 1350). This resulted in 2000 TLAT-encoding loci.

Sequence similarity network (SSN) analysis was carried out using the Enzyme Function Initiative-Enzyme Similarity Tool (EFI-EST) with input FASTA files containing all protein sequences to be analyzed.³⁸ After the initial data sets were generated, we used an alignment score that would correspond to 20% sequence identity for outputting and interpretation of the SSN. The resulting xgmml file was imported into Cytoscape 3.8.2.³⁹ Each node in the network corresponds to a single protein sequence, and each edge represents a pairwise connection between two proteins based on the specified sequence identity cutoff. The networks were visualized using the yFiles organic layout option in Cytoscape 3.8.2.

Biosynthetic gene clusters were annotated with consensus sequences generated by Geneious 10.2.2.⁴⁰

Gene Synthesis and Materials. The gene encoding EnfB (WP_098041451) from *Enterococcus faecium* strain FDAARGOS_397 was synthesized by Synbio Technologies (Suzhou). NTPs were purchased from Sigma-Aldrich. Peptides were synthesized by Chinapeptides. Q5 High-Fidelity DNA Polymerase was obtained from New England Biolabs. DNA manipulation and purification kits were purchased from Tiangen (China). Kanamycin, chloramphenicol, and other chemicals were obtained from commercial sources. Primers listed in Table S2 were purchased from RuiBiotech (Beijing, China).

Cloning, Expression, and Purification of EnfB and Its Variants. Through Gibson assembly (ThermoFisher), the gene encoding EnfB (synthesized by TransGen Biotech, China) was ligated into pET30a (Invitrogen) at the *NdeI* and *XhoI* restriction sites, with a His₆ tag introduced at the C-terminus. The resulting mixture was introduced into chemically competent TOP10 *E. coli* cells by heat shock, and cells were subsequently inoculated on solid lysogeny broth (LB) medium containing kanamycin (50 μg/mL). The plasmid was isolated from a single transformant in LB medium with kanamycin (50 μg/mL) using DNA purification kits purchased from Tiangen (China) and verified by DNA sequencing (RuiBiotech, China).

The correct plasmid was introduced into chemically competent Transetta (DE3) *E. coli* cells ((Weidi, China)) by heat shock and plated on solid LB medium supplemented with kanamycin (50 μg/mL) and chloramphenicol (34 μg/mL). LB medium (50 mL) containing kanamycin (50 μg/mL) and chloramphenicol (34 μg/mL) was inoculated with a single colony for 16 h as a preculture. Next, 2 mL of the preculture was transferred to 200 mL of LB medium (with 50 μg/mL kanamycin and 34 μg/mL chloramphenicol) and incubated at 37 °C and 200 rpm to an optical density at 600 nm of 0.6–0.8. Gene expression was induced with 0.1 mM IPTG at 16 °C and 150 rpm for 20 h. After cells were harvested by centrifugation (7000 rcf, 15 min, 4 °C), the resulting pellets were resuspended in 50 mL of lysis buffer (20 mM Tris, 500 mM NaCl, 30 mM imidazole, 10% glycerol, pH 7.4) containing hen egg white lysozyme (1 mg/mL) and incubated on ice for 10 min. Cells were lysed by an ultrahigh-pressure crusher (JNBIO, China), and insoluble components were removed by centrifugation (7000 rcf, 1 h, 4 °C). The supernatant containing recombinant protein was then filtered and loaded onto a Ni-NTA gravity flow column at 4 °C. After nonspecifically bound proteins were removed with Wash Buffer (20 mM Tris, 500 mM NaCl, 50 mM imidazole, 10% glycerol, pH 7.4), recombinant EnfB was released from the column with Elution Buffer (20 mM Tris, 500 mM NaCl, 500 mM imidazole, 10% glycerol, pH 7.4). Purified protein was exchanged into Buffer S (10 mM Tris, 200 mM NaCl, 5 mM DTT, 10% glycerol, pH 7.8) and concentrated to 5 mL in an Amicon Ultra Centrifugation Filter (10 kDa) and then further purified on a Superdex 200 column (GE) in Buffer S with a FPLC system (Bio-Rad). After size-exclusion chromatography, EnfB-containing fractions were selected by analysis on a 12% (w/v) sodium dodecyl sulfate-polyacrylamide gel electrophoresis (SDS-PAGE) gel, concentrated in an Amicon Ultra Centrifugation Filter, flash-frozen in N₂ and stored at –80 °C.

In Vitro Assays with EnfB. Chemically synthesized EnfA (200 μM, Chinapeptides) was dissolved either in phosphate buffer (0.2 M phosphate buffer, pH 7.0, 5 mM NTP, 10 mM MgCl₂) or Tris buffer (0.1 M Tris buffer, pH 7.0, 5 mM NTP, 10 mM MgCl₂) and incubated with EnfB (1.75 μM) in 100 μL of reaction mixtures at 32 °C for 3 h. Reactions were quenched by the addition of 1 μL of TFA and cleared by centrifugation

(12,000 rcf, 5 min). Supernatants (10 μ L) were then subjected to high-performance liquid chromatography (HPLC) (controller, Shimadzu CMB-20A; diode array detector, Shimadzu SPD-20A; pumps, Shimadzu LC-20A) on a reverse-phase column (SilGreen, particle size 5 μ m, 12 nm, 4.6 mm \times 250 mm) at a flow rate of 0.8 mL/min. The following gradient of solvent A (water containing 0.1% TFA) and solvent B (acetonitrile containing 0.1% TFA) was used: 20% B for 2 min, up to 45% B in 8 min, up to 95% B in 10 min, 95% B for 5 min, and 20% B in 7 min. Substrate and product concentrations were ascertained from ultraviolet (UV) peak area counts (214 nm).

For time-dependent conversion of EnfA by EnfB, *in vitro* assays were carried out as described above (with ATP as the NTP) for varying durations (0, 1, 2, 3, 4, 6, or 10 h) before quenching, clearing, and analysis. Similarly, the effect of temperature on EnfB activity was investigated over a range of 10 to 60 $^{\circ}$ C (10, 20, 30, 40, 45, 50, 55, or 60 $^{\circ}$ C) for 3 h at 600 rpm. The effect of pH on EnfB activity was likewise probed in the reaction buffer at pH values between 4.0 and 10.0 (adjusted through the addition of NaOH or HCl) for 3 h at 50 $^{\circ}$ C. Finally, the kinetic constants of EnfB were measured similarly by adding EnfB (5.46 μ M) to 100 μ L of reaction buffer containing varying concentrations of EnfA (10, 20, 30, 40, 60, 100, 200, or 500 μ M) for 3 h at 50 $^{\circ}$ C.

EnfA variants (Chinapeptides) were synthesized and, along with various primary amines, used to probe the substrate specificity of EnfB. The standard *in vitro* assays were performed as above, except with 2.72 μ M EnfB and 200 μ M EnfA variant (see Figure 5A) or one of the amines 1–6 (see Figure 5B) in place of EnfA for 12 h at 32 $^{\circ}$ C and 600 rpm before quenching, clearing, and analysis.

All experiments were conducted in triplicate.

LC-MS Analysis. Mass spectrometric analysis of the *in vitro* studies was conducted by liquid chromatography-mass spectrometry (LC-MS). For the structural analysis of the precursor and reaction products, collision-induced dissociation (CID) fragmentation was carried out using online LC-MS. To reveal the cyclization site, a Thermo Scientific Q Exactive Mass Spectrometer connected to a Thermo-Dionex (Ultimate 3000) HPLC system was employed for further MS/MS analysis. Substrates and products were separated on a homemade fused silica capillary column (75 μ m ID, 150 mm length; Upchurch Scientific) packed with C18 resin (300 Å , 5 μ m; Varian) using an isocratic elution of 20% solvent A (0.1% formic acid in water) and 80% solvent B (0.1% formic acid in acetonitrile) at a flow rate of 0.3 mL/min. XCalibur 2.1.2 software was used to control the MS instrument. A single full-scan MS in the orbitrap (100–1800 m/z , 70,000 resolution) followed by 20 data-dependent MS/MS scans at 27% normalized collision energy (higher-energy collisional dissociation, HCD) were performed. Target precursors and enzymatic products were identified and analyzed.

For LC-MS/MS analysis, samples were subjected to a Thermo-Dionex Ultimate 3000 HPLC system, which was directly interfaced with a Thermo Orbitrap Fusion Mass Spectrometer. Peptides were separated on a homemade fused silica capillary column (75 μ m ID, 150 mm length; Upchurch Scientific) packed with C18 resin (300 Å , 5 μ m; Varian) using an isocratic elution of solvent A (20%, 0.1% formic acid in water) and solvent B (80%, 0.1% formic acid in acetonitrile) at a flow rate of 0.3 μ L/min over 120 min. The Orbitrap Fusion mass spectrometer was operated in data-dependent acquisition mode using XCalibur3.0 software, allowing for a single full-scan mass

spectrum in the Orbitrap (350–1550 m/z , 120,000 resolution) followed by 3 s data-dependent MS/MS scans in an Ion Routing Multipole at 30% normalized collision energy (HCD).

Isolation and NMR Structure Elucidation of the EnfB Reaction Products. To isolate products of the EnfB reaction, *in vitro* assays were scaled up to 112 mL. A typical scaled-up reaction containing 202 μ M EnfA and 5 μ M EnfB in HEPES Buffer (50 mM HEPES, 100 mM NaCl, 5 mM ATP, 10 mM MgCl_2) was carried out for 3 h at 32 $^{\circ}$ C with shaking (800 rpm). Reactions were centrifuged and the supernatants were subjected to preparative HPLC (controller, Shimadzu CMB-20A; diode array detector; Shimadzu SPD-20A; pumps, Shimadzu LC-6AD) on a preparative reverse-phase column (SunFire C18 OBD Prep Column, 100 Å , 5 μ m, 19 mm \times 250 mm; Waters) operating at 6 mL/min, with the same solvent as for small-scale reactions. Finally, 5 mg pure products were obtained as a white powder and subjected to NMR analysis using DMSO- d_6 as the solvent.

NMR structural studies on enterofaecin were performed at the Beijing NMR Center and the NMR facility of the National Center for Protein Sciences at Peking University. All spectra were acquired with a 950 MHz Bruker NMR spectrometer. ^1H – ^1H TOCSY (60 ms mixing time) and ^1H – ^1H NOESY (150 ms mixing time) experiments were performed. The chemical shift of each proton was assigned based on intraresidue (COSY, TOCSY, HSQC) or inter-residue (NOESY) connectivities.

Structural Modeling of EnfB. To get more structural information about EnfB, AlphaFold Colab (<https://colab.research.google.com/github/deepmind/alphafold/blob/main/notebooks/AlphaFold.ipynb>), which is a simplified version of AlphaFold v2.1.0 developed by DeepMind, was selected to build the homology modeling structure of EnfB. The AlphaFold modeling studies showed that EnfB has an overall structure similar to the structure of the MccB bacterial ancestor of ubiquitin E1 (6OM4), which initiates the biosynthesis of the microcin C7 antibiotic.

RESULTS AND DISCUSSION

TLAT-Encoding Biosynthetic Pathways are Widespread in Lactic Acid Bacterial Genomes. Because RiPP natural products are assembled through a common biosynthetic logic based on conserved features,⁴¹ genome mining is an excellent approach to the discovery of previously undescribed compounds. For example, past successes targeting precursor peptides, the radical SAM or YcaO enzyme superfamilies, and even TLATs revealed that myriad “cryptic” RiPPs are yet to be discovered.^{30,42–44}

In spite of their fairly small (\sim 2 Mbp) genomes,³⁶ we hypothesized that lactic acid bacteria rely extensively on metabolites like bacteriocins to challenge competing organisms. To examine this hypothesis, we focused on TLATs, which, as demonstrated for the RiPP microcin C and pantocin A, are closely related yet versatile in their biochemical capacities.^{19,24} We suspected that mining genomes for TLATs could lead to the discovery of new RiPPs, and thus carried out PSI-BLAST searches against the sequence of MccB from the *E. coli* microcin C system (NCBI code AAY68495.1), with the organism limited to *Enterococcus* (taxid 1350) or *Streptococcus* (taxid 1301).³⁷ Next, 1000 hits from each search were grouped with the EFIEST web tool and visualized in Cytoscape.^{38,45,46}

In the resulting sequence similarity networks, hits grouped into nine (*Enterococcus*) or 11 (*Streptococcus*) distinct clades (Figures S1–S2).⁴⁷ Closer inspection of the TLAT-encoding

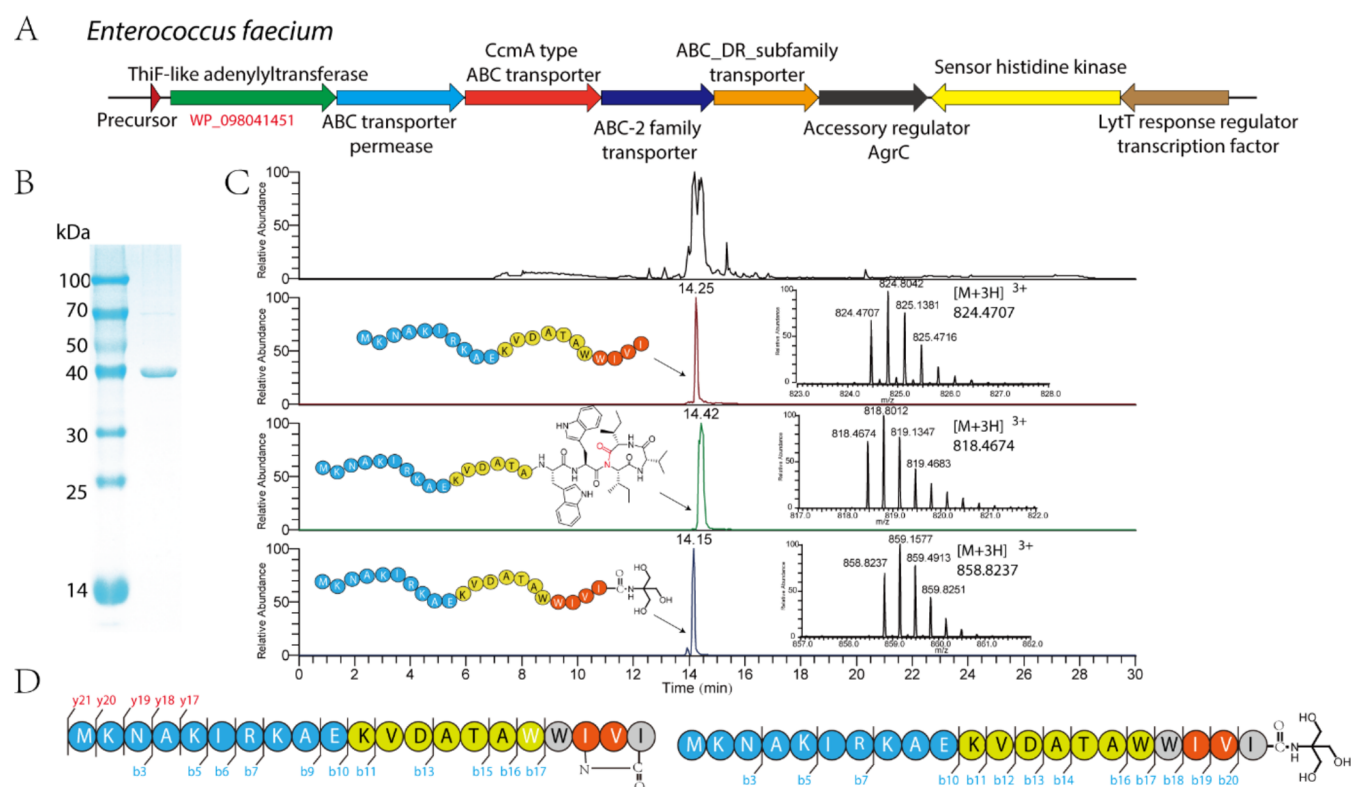


Figure 3. (A) WWIII-type cluster was identified in *E. faecalis* FDAARGOS_397 (WWIVI). (B) SDS-PAGE of the purified EnfB. Lane 1 is the protein marker and lane 2 is the final purified EnfB after size-exclusion chromatography. (C) *In vitro* cyclization and amidation of EnfA precursor peptide by EnfB, as monitored by LC-MS. Extracted ion chromatograms showing the $[M + 3H]^{3+}$ ion ($m/z = 824.4707$) of the precursor peptide, $[M + 3H]^{3+}$ ion ($m/z = 858.8237$) of the amidated peptide, and $[M + 3H]^{3+}$ ion ($m/z = 818.4674$) of the cyclized peptide. (D) Identified fragment ions are highlighted.

by gene clusters of the latter type. In both types, regulators are encoded, and the strictly conserved C-terminal residue may participate in post-translational modification, as with the VEGR type. Finally, the largest clade (with 131 hits), the GxxQY type, is the only one to code for two distinct TLATs. Aside from Bacillota, hits from the GxxQY type appear extensively in Proteobacteria (including human pathogens such as *Salmonella enterica*, *Acinetobacter baumannii*, and *Klebsiella pneumoniae*) with additional members from diverse phyla, including Aquificota, Bacterioidota, Campylobacterota, Fusobacteria, and Spirochaetota. Based on the organizations, compositions, and precursors of the above-mentioned gene clusters, our bioinformatics analyses suggest that nature employs TLATs extensively to supplement the functionality of RiPPs.

Characterization of a WWIII-Type Gene Cluster. To verify that TLATs in the identified RiPP systems can catalyze new biotransformations, we chose a WWIII-type gene cluster for further investigation. This type is dominant in *Enterococcus* and *Streptococcus* species, notably *E. faecalis* and *E. faecium*, which are commensals and opportunistic pathogens in the gastrointestinal tracts of humans,^{34,49,50} and *S. thermophilus*, which is exploited in the production of yogurt.⁵¹ Here, we focused on gene clusters from *E. faecalis* FDAARGOS_397, a species notorious for its multidrug resistance.^{50,52} The WWIII-type gene cluster encodes a 21-residue precursor peptide (EnfA, which has a WWIVI motif in this study), a TLAT (EnfB), four transporters (EnfC–F), and three enzymes involved in regulation (EnfG–I) (Table S3 and Figure 3A). Due to the lack of a leader peptidase in the gene cluster, we assumed that the final product requires its leader sequence for activity and/or cellular uptake, similar to microcin C.^{27,53} It is also possible that a potential peptidase located in

another region of the genome could be responsible for the removal of the leader peptide. However, this hypothesis needs to be confirmed in future research.

To assess the TLAT reaction, we purchased the precursor peptide EnfA prepared by solid-phase peptide synthesis; the TLAT EnfB was heterologously expressed in *E. coli* with a C-terminal His₆ tag and purified via Ni-NTA and size-exclusion chromatography (Figure S3 and 3B). EnfA and EnfB were then incubated together in the presence of an ATP, CTP, UTP, or GTP cosubstrate in Tris buffer and monitored by HPLC. While no change was observed in reactions containing CTP or GTP, two new peptide species appeared when ATP or UTP was included (although efficiency was higher for ATP) (Figure S4). This observation resembles that made with MccB from *E. coli* and *B. amyloliquefaciens*, which favor ATP and CTP, respectively, but are able to modify their precursor peptide in the presence of any of the four NTPs.²⁸ In the biosynthesis of microcin C, a peptidyl-succinimide intermediate was observed.²⁴ We also anticipated the formation of an intermediate in our reaction, which would explain the presence of two new species.

MS and NMR Analyses Reveal a Novel Cyclization-Type Post-Translational Modification. To determine the identity of the peptide products observed in our EnfB activity assays, we carried out a high-resolution MS/MS analysis. Relative to native EnfA ($[M + 3H]^{3+}$ calc: 824.4701, $[M + 3H]^{3+}$ obs: 824.4707), one product showed loss of water ($[M + 3H]^{3+}$ obs: 818.4674, $[M + 3H]^{3+}$ calc: 818.4666), suggesting that EnfB promotes intramolecular cyclization of the peptide (Figure 3C and S5).²⁴ Although we could observe most of the b-ion fragments for the substrate, fragmentation was not detected

within the final four residues of the product, pointing to one of those residues and the terminal carboxyl group as the likely sites of cyclization (Figures 3D and S6). The second product was differently modified, not with an adenylyl group but a Tris group ($[M + 3H]^{3+}$ obs: 858.8237, $[M + 3H]^{3+}$ calc: 858.8245). Indeed, when Tris was omitted from the assays, the modification was absent from EnfA (Figure S7).

To confirm our hypothesis, further LC-MS/MS analysis was performed on a Thermo Scientific Q Exactive Mass Spectrometer, and a similar result was obtained. The observation of the b18 ions in both native EnfA and Tris-modified EnfA and the absence of b18 ions in the cyclic product are consistent with the previous observation, which provided a fragmentation pattern indicative of cross-link formation at the C-terminal WIVI motif (Figure S6). We then used a Thermo Orbitrap Fusion mass spectrometer to perform an additional MS/MS analysis. Both the linear and C-terminal modified peptides have clear series b fragments, including b17, b18, b19, and b20 fragments, which demonstrate that the modification occurred at the C-terminus (Figures S8–S9). On the other hand, the cyclic peptide has different spectra and shows several y fragments, including y17, y18, y19, and y20. Further MS³ analysis on the y19²⁺ fragment showed that b15 is clearly present, but no b16 could be detected, which further proves the cyclization position (Figure S10).

To further pinpoint the position of the EnfB-catalyzed cyclization, structure elucidation was conducted via NMR spectroscopy. Scaling up of *in vitro* assays and purification by preparative HPLC resulted in 2 mg of cyclized peptides (Figure S11), which were subjected to extensive NMR analysis (Figures S12–S15). We were able to completely assign resonances to the linear EnfA substrate (Table S4); in contrast, the assignment of the product resonances was more challenging due to spontaneous hydrolysis. In the substrate spectra, two typical indole signals (10.24 and 10.04 ppm) were apparent for Trp17 and Trp18. In the product spectra, these signals were likewise present (Figure S16), which ruled out the possibility of an isopeptide bond involving the indole amine of either Trp side chain and instead suggested an imide bond between the Ile19 backbone N atom and the C-terminus. These results, combined with our MS analysis, suggest that EnfB not only installs macrocyclic imides in peptides but also activates their C-termini for modification. However, since the NMR analysis of the cyclization products has not been fully resolved, further research is necessary to confirm their detailed structural information.

Biochemical Characterization of EnfB. EnfB-catalyzed conversion of EnfA was subsequently characterized *in vitro* through time course analysis in phosphate buffer by HPLC. After 6 h, ~50% of the precursor (200 μ M) was transformed into a macrolactam by 1.75 μ M EnfB (Figure S17). Increasing the reaction duration failed to improve conversion significantly, likely due to enzyme instability (a white precipitate became visible during the assays). Therefore, incubation for 3 h was selected for further optimization. Interestingly, we observed a steady increase in EnfB activity with temperature from 10 to 50 $^{\circ}$ C, with a decline to nil by 60 $^{\circ}$ C. EnfB thus exhibits modest thermostability and processes its substrate most efficiently at a temperature significantly higher than that for optimal growth of *E. faecalis* (Figure S18A). We also tested the effect of pH on EnfB activity over a range of 4.0 to 10.0 (at 50 $^{\circ}$ C), resulting in a maximum at pH 7.0 (Figure S18B). Finally, the kinetics with respect to EnfA concentration were evaluated at the optimal pH and temperature, resulting in apparent $K_m = 58 \pm 15 \mu$ M, $k_{cat} =$

$0.072 \pm 0.007 \text{ min}^{-1}$, and $k_{cat}/K_m = 0.001 \text{ min}^{-1} \mu\text{M}^{-1}$ (Figure 4A).

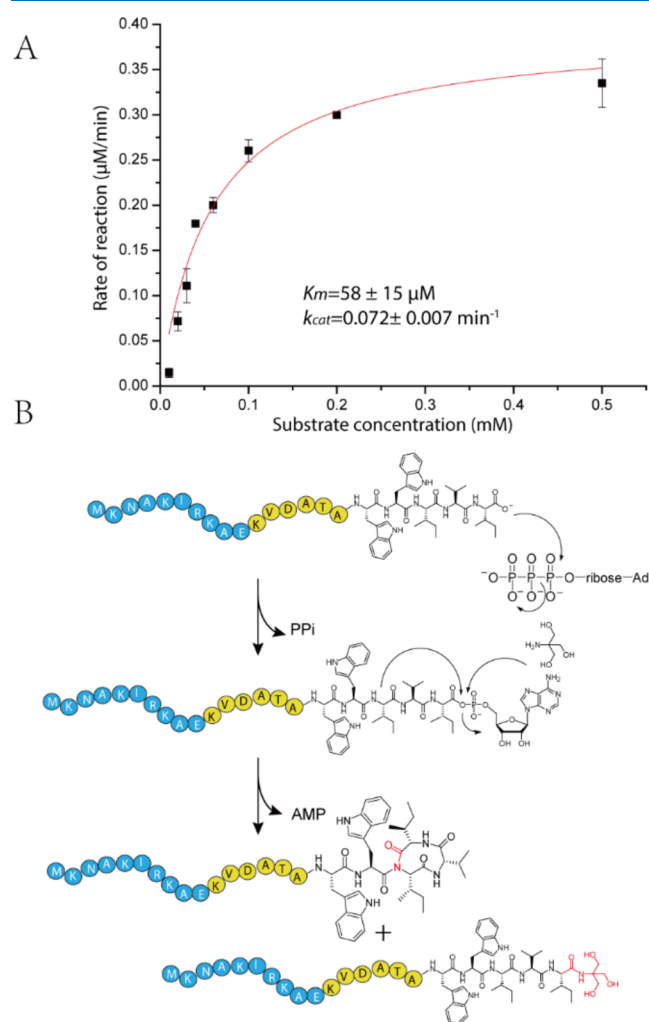


Figure 4. (A) Kinetic characterization of the cyclization catalyzed by EnfB. (B) proposed mechanism of EnfB-catalyzed cyclization and amidation of the C-terminal of a precursor peptide. After activation by ATP, the C-terminal acyl-AMP anhydride of EnfA is attacked either by the nitrogen from the peptide bond at Ile19 to form a macrocyclic imide or by the nitrogen in small organic molecules to amidate the C-terminus.

Proposed Catalytic Mechanism of EnfB. Based on the consumption of ATP and formation of two products in our assays with EnfB (Figure 3C), the reaction likely resembles that of MccB, which catalyzes C-terminal adenylation of its precursor peptide followed by intramolecular cyclization and subsequent ring opening.²⁴ To compare the structures of these two enzymes (EnfB 22% identical in sequence to MccB), we predicted its structure with the neural network AlphaFold (Figure S19).^{54,55}

As observed for MccB and PaaA, the EnfB model consists of two subdomains: an N-terminal RIPP recognition element (RRE) domain and a C-terminal adenylation domain that bind and modify the precursor peptide leader and core sequences, respectively.^{11,19} Superposition of the EnfB model with the structure of MccB bound to ATP and Mg²⁺ (PDB ID: 6OM4) allowed the roles of key residues to be predicted. Arg167 and Lys180 are highly conserved among reported TLATs due to their essential role in ATP binding.^{11,19,56} When we substituted

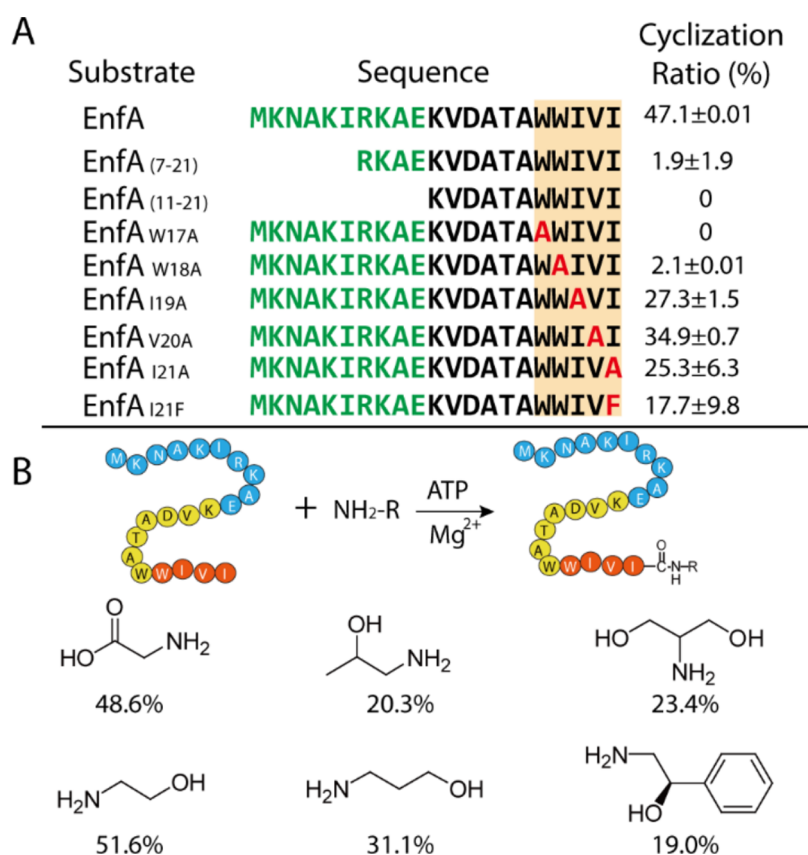


Figure 5. (A) Results of substrate specificity assays with EnfB and EnfA analogues. (B) Results of substrate specificity assays with EnfB and the amino compounds. The cyclization ratio or the amidation ratio was shown alongside.

these residues with Ala, EnfB was found to be insoluble. Asp225, another conserved residue, is expected to coordinate the Mg²⁺ ion that stabilizes the negative charge of ATP. Ala mutagenesis likewise showed that this residue is essential, as no conversion of EnfA was detected. Moreover, an ordered “lid” motif, not modeled in the MccB structure, was observed above the putative substrate binding pocket.

On the basis of the structural information, we proposed that EnfB employed a similar catalytic mechanism for C-terminal carboxyl activation of EnfA but a different process for further post-translational modification. While MccB requires two moles of ATP for N–P bond formation, EnfB only consumes one mole of ATP for cyclization and amidation.²⁴ The first stage is similar, whereas the C-terminus carboxylate attacks P_α of the ATP, yielding a hydrolytically labile precursor-CO-AMP. In the modification of MccA, the carboxamido nitrogen of Asn7 first attacks the C-terminal acyl-AMP anhydride to form a succinimide intermediate, then a second ATP is consumed to form the unusual N–P bond to synthesize the unprocessed microcin C. On the other hand, there is a different scenario for enterofaecin biosynthesis. The C-terminal acyl-AMP anhydride of EnfA was attacked either by the nitrogen from the peptide bond at Ile19 to form a macrocyclic imide or by the nitrogen contained in small organic molecules present in the medium to amidate the C-terminus (Figure 4B).

Substrate Specificity of EnfB. We next investigated the substrate specificity of EnfB. Given that RiPP biosynthesis is guided by the leader sequence, we wondered whether the enterofaecin system would comply with the same rules.⁴⁸ Two N-terminal truncations, EnfA_(11–21) and EnfA_(7–21), which lack a conserved (V/I)RKA motif in the leader sequence and all

residues N-terminal to that motif, respectively, were prepared (Figures 2A and 5A). Following incubation with EnfB for 3 h, no or minor conversion was observed by LC-MS analysis, which was in agreement with the role of the putative N-terminal RRE domain of EnfB in binding the leader sequence.

We next probed the roles of Trp17 and Trp18 in the core sequence, which are conserved in many of the identified gene clusters of the WWIII type. Substitution of Trp17 or Trp18 with Ala completely abolished conversion or decreased it to 2.1%, suggesting that these residues are likely involved in substrate recognition by the adenylation domain of EnfB. We considered whether the substitution of residues in the ring structure would disrupt enzymatic processing. The variants EnfA_{I19A}, EnfA_{V20A}, EnfA_{I21A}, and EnfA_{I21F} were generated and individually incubated with EnfB as before. As yields ranged from 17.7–34.9% for these variants, EnfB is apparently relaxed in specificity toward the three C-terminal positions of EnfA (Figures 5A and S20–S23).

As noted above, we observed C-terminal amidation of EnfA with Tris when assays with EnfB were carried out in a Tris buffer. To further probe the substrate scope of the enzyme, we assayed a small set of primary amines: glycine (1), isopropanolamine (2), serinol (3), ethanolamine (4), propanolamine (5), and (*R*)-phenylethanolamine (6) (Figure 5B). Interestingly, EnfB was able to catalyze the amidation of EnfA with all six of these compounds (Figures 5B and S24–S29). Coupled with the presence of a multitude of primary amines in the cell, this activity may explain why multiple transporters are encoded in the enterofaecin gene cluster.

Evolution of Isopeptide Macrocyclase. Our genome mining efforts revealed that TLAT-RiPP pathways are widely

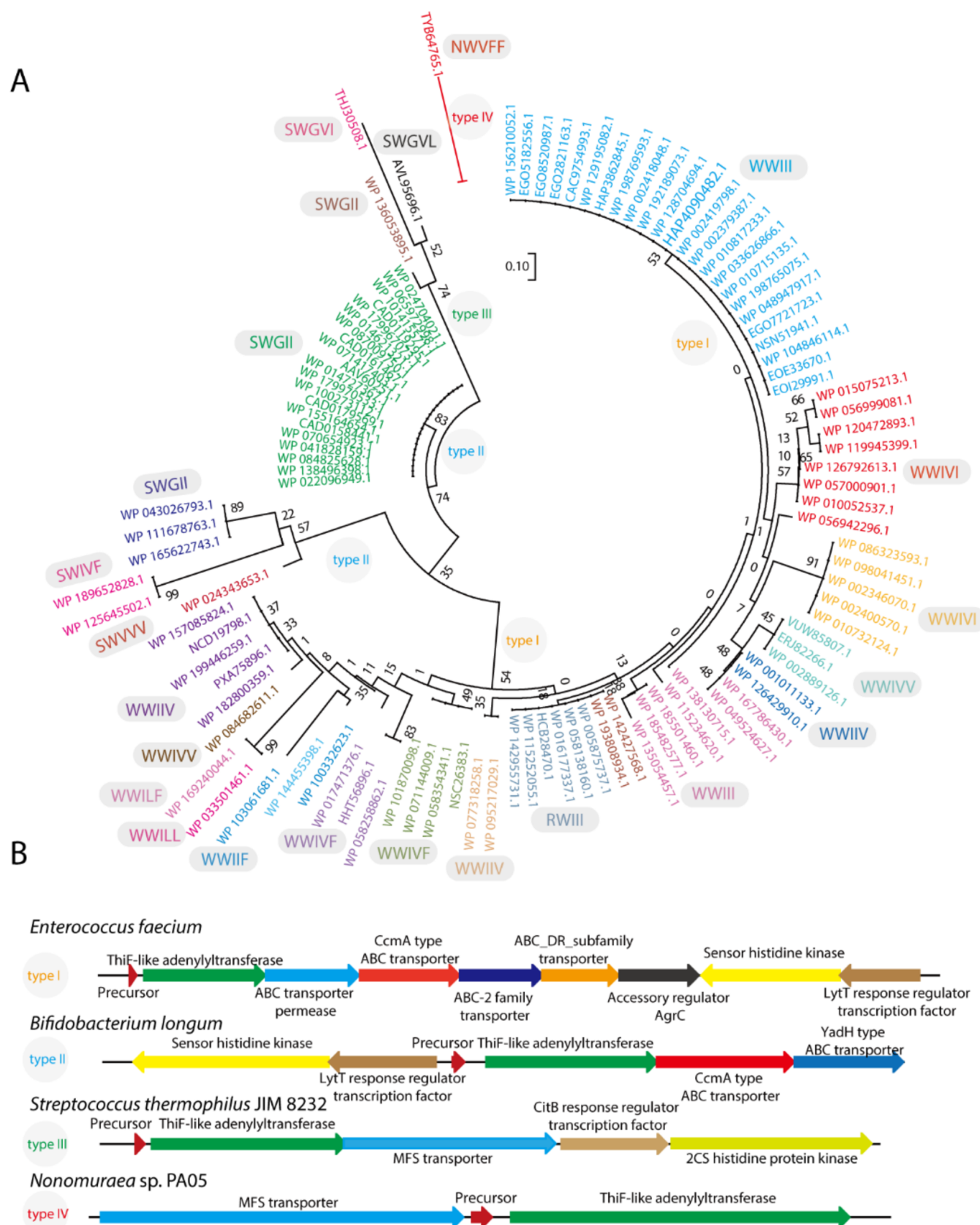


Figure 6. (A) Evolution of the precursor peptide for these diverse macrocyclase. The substrates could be classified into 4 clades based on the organization of their biosynthetic gene clusters. (B) Representative biosynthetic gene cluster for each of the subfamilies in panel (A).

present in nature. For example, the WWIII type is utilized by a range of Bacillota (including lactic acid bacteria) and Actino-

mycetota. To study the evolutionary patterns of this type of system, we prepared a phylogenetic distribution of precursor

RiPPs make up a rapidly growing family of natural products with a mechanistically distinct logic and enzymatic machinery for cyclization. The subcategories of RiPPs have expanded greatly due to the explosion of genomic data and the development of novel bioinformatics approaches. While past research has intensively focused on talented genera for natural product discovery, bacterial genera with small genomes, such as Lactobacillales, have frequently been overlooked.⁶² We herein significantly expand the ThiF-RiPP family of natural products through genome mining in *Lactobacillales* and have systematically identified diverse ThiF-RiPP groups based on the type of biosynthetic pathways and conserved precursor sequences. This bioinformatics survey, based on a sequence similarity network limited to one genus, revealed a phylogenetically distinct yet unexpected subgroup of biosynthetic machinery that might be a rich source for novel natural products with completely new scaffolds. Focusing on one system from *E. faecalis* FDAARGOS_397 identified in the network, we demonstrated a unique logic to form constraining macrocyclic imides in diverse peptides. This discovery provides a remarkably efficient strategy to assemble peptides into highly compact macrocyclic frameworks. Previously, peptide macrolactam frameworks were frequently synthesized via large NRPS machinery, which uses thioesterase domains to mediate macrocyclic formation.⁵⁹ Macrolactam construction mediated by ATP is found in only a few RiPP families, such as lasso peptides and ω -ester-containing peptides.^{63,64} However, the reaction of EnfB described here is the first known imide macrocyclase that specifically catalyzes the cyclization of its precursor peptide by connecting a conserved WI(V)I(V)I(V) motif at the C-terminus through macrocyclic imide formation. Considering that lactam-type natural products remain the mainstays of antibiotic therapy, this unique biochemical logic and post-translational enzymatic machinery could be of great utility in creating diverse arrays of macrocyclic imide structures.

In conclusion, this article establishes a foundation for further study of novel ThiF-RiPP-type natural product biosynthesis, within which many intriguing questions remain. The WWIII system described herein produces both cyclic and C-terminally amidated products that likely require different transporter types for export. Thus far, the function of these peptide molecules remains unknown. The association of the accessory regulator AgrC, the sensor histidine kinase, and the LytT response regulator transcription factor genes suggests that they might be involved in quorum sensing (Figure 7).⁶⁵ Given that diverse species of *Streptococcus* and *Enterococcus* are also pathogens, this potential quorum sensing (QS) system is of great interest, especially since several prevalent human pathogens, such as *S. aureus*, use QS to regulate virulence.^{65,66} The QS system could be developed as a novel target for anti-infective therapies. Therefore, the investigation into the biosynthesis of the novel macrolactam analogues presented here offers a new opportunity for the development of non-native ligands that can interact with such QS pathways.

In addition to the system characterized here, the discovery of diverse ThiF-RiPP gene clusters within the *Lactobacillales* order necessitates further exploration to identify the mature end products of these pathways. Such products warrant additional investigations to elucidate their chemical structures and biological functions. We believe that more rigorous bioinformatics analyses will reveal additional novel RiPP groups possessing distinct structures and properties, thereby offering insights into biosynthetic mechanisms and various tailoring

modifications. Focusing exclusively on ThiF-RiPP-type natural products in *Streptococcus* and *Enterococcus* has proven fruitful, uncovering novel systems that may represent only the tip of the iceberg. Future research into other genera, targeting ThiF and other biosynthetic enzymes such as those in the YcaO and RaS families, will very probably provide significant opportunities for discovering novel RiPPs and deepening our understanding of the underlying biology, chemistry, and enzymology in the years ahead.

■ ASSOCIATED CONTENT

SI Supporting Information

The Supporting Information is available free of charge at <https://pubs.acs.org/doi/10.1021/acsomega.4c03760>.

Lists the primers used (Table S2); the proposed functions of ORFs in the RiPP BGC (Table S3); assigns the ¹H NMR signals (ppm) of linear EnfA (Table S4); depict the network of RiPP BGCs from the Lactobacillales order utilizing adenylyltransferases (Figures S1 and S2); the purification of EnfB (Figure S3); illustrate the *in vitro* assays with EnfB and different NTPs (Figures S4–S10); demonstrates the purification of cyclic products (Figure S11); the NMR spectra of EnfA and its modified products (Figures S12–S16); biochemical characterization of EnfB (Figures S17 and S18); the AlphaFold homology model of EnfB (Figure S19); the substrate specificity of EnfB (Figures S20 to S29), and reveal the potential quorum sensing (QS) role of the identified RiPP BGCs (Figures S30 and S31) (PDF)

RiPP BGCs from the Lactobacillales order utilizing a TLAT (XLSX)

Accession Codes

The *EnfB* gene from *E. faecalis* FDAARGOS_397 strain (Accession number: WP_098041451.1).

■ AUTHOR INFORMATION

Corresponding Authors

Aili Fan – State Key Laboratory of Natural and Biomimetic Drugs, Peking University, Beijing 100191, People's Republic of China; Phone: +86-10-64431557; Email: fanaili@bjmu.edu.cn

Shaozhou Zhu – National Institutes for Food and Drug Control, Beijing 102629, People's Republic of China; orcid.org/0000-0003-3106-4085; Phone: +86-10-64431557; Email: zhusz@nifdc.org.cn

Yigang Tong – College of Life Science and Technology, Beijing University of Chemical Technology, Beijing 100029, People's Republic of China; Phone: +86-10-64431557; Email: tong.yigang@gmail.com

Authors

Mengjiao Wang – College of Life Science and Technology, Beijing University of Chemical Technology, Beijing 100029, People's Republic of China

Mengyue Wu – State Key Laboratory of Natural and Biomimetic Drugs, Peking University, Beijing 100191, People's Republic of China

Meng Han – MOE Key Laboratory of Bioinformatics, School of Life Sciences, Tsinghua University, Beijing 100084, People's Republic of China

Xiaogang Niu – Beijing Nuclear Magnetic Resonance Center,
College of Chemistry and Molecular Engineering, Peking
University, Beijing 100871, People's Republic of China

Complete contact information is available at:
<https://pubs.acs.org/10.1021/acsomega.4c03760>

Author Contributions

[#]M.Wang and M.Wu contributed equally to this work. S.Z., A.F., and Y.T.: Conceptualization, supervision, and writing. M.Wang, M.Wu, M.H., and X.N.: Investigation and methodology. All authors have given approval to the final version of the manuscript.

Notes

The authors declare no competing financial interest.

ACKNOWLEDGMENTS

Financial support from the Natural Science Foundation of Beijing Municipality (No. 7202107), the National Natural Science Foundation of China (NSFC; Grant No. 21706005), the National Key Research and Development Program of China (2022YFC2804900), and the State Key Laboratory of Drug Regulatory Science (2023SKLDRS0109) are gratefully acknowledged. All NMR experiments were carried out at the Beijing NMR Center and the NMR facility of the National Center for Protein Sciences at Peking University.

REFERENCES

- (1) Montalbán-López, M.; Scott, T. A.; Ramesh, S.; Rahman, I. R.; van Heel, A. J.; Viel, J. H.; Bandarian, V.; Dittmann, E.; Genilloud, O.; Goto, Y.; Burgos, M. J. G.; Hill, C.; Kim, S.; Koehnke, J.; Latham, J. A.; Link, A. J.; Martínez, B.; Nair, S. K.; Nicolet, Y.; Rebuffat, S.; Sahl, H.-G.; Sareen, D.; Schmidt, E. W.; Schmitt, L.; Severinov, K.; Süßmuth, R. D.; Truman, A. W.; Wang, H.; Weng, J.-K.; van Wezel, G. P.; Zhang, Q.; Zhong, J.; Piel, J.; Mitchell, D. A.; Kuipers, O. P.; van der Donk, W. A. New developments in RiPP discovery, enzymology and engineering. *Nat. Prod. Rep.* **2021**, *38*, 130–239.
- (2) Ongpipattanakul, C.; Desormeaux, E. K.; DiCaprio, A.; van der Donk, W. A.; Mitchell, D. A.; Nair, S. K. Mechanism of Action of Ribosomally Synthesized and Post-Translationally Modified Peptides. *Chem. Rev.* **2022**, *122*, 14722–14814.
- (3) Ortega, M. A.; van der Donk, W. A. New Insights into the Biosynthetic Logic of Ribosomally Synthesized and Post-translationally Modified Peptide Natural Products. *Cell Chem. Biol.* **2016**, *23*, 31–44.
- (4) Truman, A. W. Cyclisation mechanisms in the biosynthesis of ribosomally synthesised and post-translationally modified peptides. *Beilstein J. Org. Chem.* **2016**, *12*, 1250–1268.
- (5) Dunbar, K. L.; Melby, J. O.; Mitchell, D. A. YcaO domains use ATP to activate amide backbones during peptide cyclodehydrations. *Nat. Chem. Biol.* **2012**, *8*, 569–575.
- (6) Dunbar, K. L.; Mitchell, D. A. Insights into the mechanism of peptide cyclodehydrations achieved through the chemoenzymatic generation of amide derivatives. *J. Am. Chem. Soc.* **2013**, *135*, 8692–8701.
- (7) Xie, L.; Miller, L. M.; Chatterjee, C.; Averin, O.; Kelleher, N. L.; van der Donk, W. A. Lactacin 481: in vitro reconstitution of lantibiotic synthetase activity. *Science* **2004**, *303*, 679–681.
- (8) Clarke, D. J.; Campopiano, D. J. Maturation of McjA precursor peptide into active microcin MccJ25. *Org. Biomol. Chem.* **2007**, *5*, 2564–2566.
- (9) Duquesne, S.; Destoumieux-Garzon, D.; Zirah, S.; Goulard, C.; Peduzzi, J.; Rebuffat, S. Two enzymes catalyze the maturation of a lasso peptide in *Escherichia coli*. *Chem. Biol.* **2007**, *14*, 793–803.
- (10) Philmus, B.; Christiansen, G.; Yoshida, W. Y.; Hemscheidt, T. K. Post-translational modification in microviridin biosynthesis. *ChemBioChem* **2008**, *9*, 3066–3073.
- (11) Regni, C. A.; Roush, R. F.; Miller, D. J.; Nourse, A.; Walsh, C. T.; Schulman, B. A. How the MccB bacterial ancestor of ubiquitin E1 initiates biosynthesis of the microcin C7 antibiotic. *EMBO J.* **2009**, *28*, 1953–1964.
- (12) Dunbar, K. L.; Tietz, J. I.; Cox, C. L.; Burkhart, B. J.; Mitchell, D. A. Identification of an Auxiliary Leader Peptide-Binding Protein Required for Azoline Formation in Ribosomal Natural Products. *J. Am. Chem. Soc.* **2015**, *137*, 7672–7677.
- (13) Schulman, B. A.; Harper, J. W. Ubiquitin-like protein activation by E1 enzymes: the apex for downstream signalling pathways. *Nat. Rev. Mol. Cell Biol.* **2009**, *10*, 319–331.
- (14) Burkhart, B. J.; Hudson, G. A.; Dunbar, K. L.; Mitchell, D. A. A prevalent peptide-binding domain guides ribosomal natural product biosynthesis. *Nat. Chem. Biol.* **2015**, *11*, 564–570.
- (15) Dunbar, K. L.; Chekan, J. R.; Cox, C. L.; Burkhart, B. J.; Nair, S. K.; Mitchell, D. A. Discovery of a new ATP-binding motif involved in peptidic azoline biosynthesis. *Nat. Chem. Biol.* **2014**, *10*, 823–829.
- (16) Koehnke, J.; Bent, A. F.; Zollman, D.; Smith, K.; Houssen, W. E.; Zhu, X.; Mann, G.; Lebl, T.; Scharff, R.; Shirran, S.; Botting, C. H.; Jaspars, M.; Schwarz-Linek, U.; Naismith, J. H. The Cyanobactin Heterocyclase Enzyme: A Processive Adenylase That Operates with a Defined Order of Reaction. *Angew. Chem., Int. Ed.* **2013**, *52*, 13991–13996.
- (17) Koehnke, J.; Mann, G.; Bent, A. F.; Ludewig, H.; Shirran, S.; Botting, C.; Lebl, T.; Houssen, W.; Jaspars, M.; Naismith, J. H. Structural analysis of leader peptide binding enables leader-free cyanobactin processing. *Nat. Chem. Biol.* **2015**, *11*, 558–563.
- (18) Ghilarov, D.; Stevenson, C. E. M.; Travin, D. Y.; Piskunova, J.; Serebryakova, M.; Maxwell, A.; Lawson, D. M.; Severinov, K. Architecture of Microcin B17 Synthetase: An Octameric Protein Complex Converting a Ribosomally Synthesized Peptide into a DNA Gyrase Poison. *Mol. Cell* **2019**, *73*, 749–762.e5.
- (19) Ghodge, S. V.; Biernat, K. A.; Bassett, S. J.; Redinbo, M. R.; Bowers, A. A. Post-translational Claisen Condensation and Decarboxylation en Route to the Bicyclic Core of Pantocin A. *J. Am. Chem. Soc.* **2016**, *138*, 5487–5490.
- (20) Jin, M.; Wright, S. A.; Beer, S. V.; Clardy, J. The biosynthetic gene cluster of Pantocin A provides insights into biosynthesis and a tool for screening. *Angew. Chem., Int. Ed.* **2003**, *42*, 2902–2905.
- (21) Jin, M.; Liu, L.; Wright, S. A.; Beer, S. V.; Clardy, J. Structural and functional analysis of pantocin A: an antibiotic from *Pantoea agglomerans* discovered by heterologous expression of cloned genes. *Angew. Chem., Int. Ed.* **2003**, *42*, 2898–2901.
- (22) González-Pastor, J. E.; Millán, J. L. S.; Castilla, M. A.; Moreno, F. Structure and organization of plasmid genes required to produce the translation inhibitor microcin C7. *J. Bacteriol.* **1995**, *177*, 7131–7140.
- (23) Metlitskaya, A.; Kazakov, T.; Kommer, A.; Pavlova, O.; Praetorius-Ibba, M.; Ibba, M.; Krashennikov, I.; Kolb, V.; Khmel, I.; Severinov, K. Aspartyl-tRNA synthetase is the target of peptide nucleotide antibiotic Microcin C. *J. Biol. Chem.* **2006**, *281*, 18033–18042.
- (24) Roush, R. F.; Nolan, E. M.; Lohr, F.; Walsh, C. T. Maturation of an *Escherichia coli* ribosomal peptide antibiotic by ATP-consuming N-P bond formation in microcin C7. *J. Am. Chem. Soc.* **2008**, *130*, 3603–3609.
- (25) Kulikovskiy, A.; Serebryakova, M.; Bantysh, O.; Metlitskaya, A.; Borukhov, S.; Severinov, K.; Dubiley, S. The molecular mechanism of aminopropylation of peptide-nucleotide antibiotic microcin C. *J. Am. Chem. Soc.* **2014**, *136*, 11168–11175.
- (26) Tikhonov, A.; Kazakov, T.; Semenova, E.; Serebryakova, M.; Vondenhoff, G.; Van Aerschot, A.; Reader, J. S.; Govorun, V. M.; Severinov, K. The mechanism of microcin C resistance provided by the MccF peptidase. *J. Biol. Chem.* **2010**, *285*, 37944–37952.
- (27) Severinov, K.; Nair, S. K. Microcin C: biosynthesis and mechanisms of bacterial resistance. *Future Microbiol.* **2012**, *7*, 281–289.
- (28) Serebryakova, M.; Tsibulskaya, D.; Mokina, O.; Kulikovskiy, A.; Nautiyal, M.; Van Aerschot, A.; Severinov, K.; Dubiley, S. A Trojan-Horse Peptide-Carboxymethyl-Cytidine Antibiotic from *Bacillus amyloliquefaciens*. *J. Am. Chem. Soc.* **2016**, *138*, 15690–15698.

- (29) Severinov, K.; Semenova, E.; Kazakov, A.; Kazakov, T.; Gelfand, M. S. Low-molecular-weight post-translationally modified microcins. *Mol. Microbiol.* **2007**, *65*, 1380–1394.
- (30) Bantysh, O.; Serebryakova, M.; Makarova, K. S.; Dubiley, S.; Datsenko, K. A.; Severinov, K. Enzymatic synthesis of bioinformatically predicted microcin C-like compounds encoded by diverse bacteria. *mBio* **2014**, *5*, No. e01059-14.
- (31) Johnson, B. A.; Clark, K. A.; Bushin, L. B.; Spolar, C. N.; Seyedsayamdost, M. R. Expanding the Landscape of Noncanonical Amino Acids in RiPP Biosynthesis. *J. Am. Chem. Soc.* **2024**, *146*, 3805–3815.
- (32) Wang, Y.; Wu, J.; Lv, M.; Shao, Z.; Hungwe, M.; Wang, J.; Bai, X.; Xie, J.; Wang, Y.; Geng, W. Metabolism Characteristics of Lactic Acid Bacteria and the Expanding Applications in Food Industry. *Front. Bioeng. Biotechnol.* **2021**, *9*, No. 612285.
- (33) Wu, Y.; Pang, X.; Wu, Y.; Liu, X.; Zhang, X. Enterocins: Classification, Synthesis, Antibacterial Mechanisms and Food Applications. *Molecules* **2022**, *27*, No. 2258.
- (34) Nobbs, A. H.; Lamont, R. J.; Jenkinson, H. F. *Streptococcus* Adherence and Colonization. *Microbiol. Mol. Biol. Rev.* **2009**, *73*, 407–450.
- (35) Baltz, R. H. Gifted microbes for genome mining and natural product discovery. *J. Ind. Microbiol. Biotechnol.* **2017**, *44*, 573–588.
- (36) Schroeter, J.; Klaenhammer, T. Genomics of lactic acid bacteria. *FEMS Microbiol. Lett.* **2009**, *292*, 1–6.
- (37) Altschul, S. F.; Madden, T. L.; Schäffer, A. A.; Zhang, J.; Zhang, Z.; Miller, W.; Lipman, D. J. Gapped BLAST and PSI-BLAST: a new generation of protein database search programs. *Nucleic Acids Res.* **1997**, *25*, 3389–3402.
- (38) Zallot, R.; Oberg, N.; Gerlt, J. A. The EFI Web Resource for Genomic Enzymology Tools: Leveraging Protein, Genome, and Metagenome Databases to Discover Novel Enzymes and Metabolic Pathways. *Biochemistry* **2019**, *58*, 4169–4182.
- (39) Shannon, P.; Markiel, A.; Ozier, O.; Baliga, N. S.; Wang, J. T.; Ramage, D.; Amin, N.; Schwikowski, B.; Ideker, T. Cytoscape: a software environment for integrated models of biomolecular interaction networks. *Genome Res.* **2003**, *13*, 2498–2504.
- (40) Kearse, M.; Moir, R.; Wilson, A.; Stones-Havas, S.; Cheung, M.; Sturrock, S.; Buxton, S.; Cooper, A.; Markowitz, S.; Duran, C.; Thierer, T.; Ashton, B.; Meintjes, P.; Drummond, A. Geneious Basic: An integrated and extendable desktop software platform for the organization and analysis of sequence data. *Bioinformatics* **2012**, *28*, 1647–1649.
- (41) Arnison, P. G.; Bibb, M. J.; Bierbaum, G.; Bowers, A. A.; Bugni, T. S.; Bulaj, G.; Camarero, J. A.; Campopiano, D. J.; Challis, G. L.; Clardy, J.; Cotter, P. D.; Craik, D. J.; Dawson, M.; Dittmann, E.; Donadio, S.; Dorrestein, P. C.; Entian, K. D.; Fischbach, M. A.; Garavelli, J. S.; Goransson, U.; Gruber, C. W.; Haft, D. H.; Hemscheidt, T. K.; Hertweck, C.; Hill, C.; Horswill, A. R.; Jaspars, M.; Kelly, W. L.; Klinman, J. P.; Kuipers, O. P.; Link, A. J.; Liu, W.; Marahiel, M. A.; Mitchell, D. A.; Moll, G. N.; Moore, B. S.; Muller, R.; Nair, S. K.; Nes, I. F.; Norris, G. E.; Olivera, B. M.; Onaka, H.; Patchett, M. L.; Piel, J.; Reaney, M. J.; Rebuffat, S.; Ross, R. P.; Sahl, H. G.; Schmidt, E. W.; Selsted, M. E.; Severinov, K.; Shen, B.; Sivonen, K.; Smith, L.; Stein, T.; Sussmuth, R. D.; Tagg, J. R.; Tang, G. L.; Truman, A. W.; Vederas, J. C.; Walsh, C. T.; Walton, J. D.; Wenzel, S. C.; Willey, J. M.; van der Donk, W. A. Ribosomally synthesized and post-translationally modified peptide natural products: overview and recommendations for a universal nomenclature. *Nat. Prod. Rep.* **2013**, *30*, 108–160.
- (42) Burkhart, B. J.; Schwalen, C. J.; Mann, G.; Naismith, J. H.; Mitchell, D. A. YcaO-Dependent Posttranslational Amide Activation: Biosynthesis, Structure, and Function. *Chem. Rev.* **2017**, *117*, 5389–5456.
- (43) Bushin, L. B.; Clark, K. A.; Pelczar, I.; Seyedsayamdost, M. R. Charting an Unexplored *Streptococcal* Biosynthetic Landscape Reveals a Unique Peptide Cyclization Motif. *J. Am. Chem. Soc.* **2018**, *140*, 17674–17684.
- (44) Tietz, J. I.; Schwalen, C. J.; Patel, P. S.; Maxson, T.; Blair, P. M.; Tai, H. C.; Zakai, U. I.; Mitchell, D. A. A new genome-mining tool redefines the lasso peptide biosynthetic landscape. *Nat. Chem. Biol.* **2017**, *13*, 470–478.
- (45) Gerlt, J. A.; Bouvier, J. T.; Davidson, D. B.; Imker, H. J.; Sadkhin, B.; Slater, D. R.; Whalen, K. L. Enzyme Function Initiative-Enzyme Similarity Tool (EFI-EST): A web tool for generating protein sequence similarity networks. *Biochim. Biophys. Acta, Proteins Proteomics* **2015**, *1854*, 1019–1037.
- (46) Su, G.; Morris, J. H.; Demchak, B.; Bader, G. D. Biological Network Exploration with Cytoscape 3. *Curr. Protoc. Bioinf.* **2014**, *47*, 8.13.1–8.13.24.
- (47) Song, N.; Joseph, J. M.; Davis, G. B.; Durand, D. Sequence similarity network reveals common ancestry of multidomain proteins. *PLoS Comput. Biol.* **2008**, *4*, No. e1000063.
- (48) Ortega, M. A.; van der Donk, W. A. New Insights into the Biosynthetic Logic of Ribosomally Synthesized and Post-translationally Modified Peptide Natural Products. *Cell Chem. Biol.* **2016**, *23*, 31–44.
- (49) Murray, B. E. The life and times of the Enterococcus. *Clin. Microbiol. Rev.* **1990**, *3*, 46–65.
- (50) Fiore, E.; Van Tyne, D.; Gilmore, M. S. Pathogenicity of *Enterococci*. *Microbiol. Spectrum* **2019**, *74* DOI: 10.1128/microbiolspec.GPP3-0053-2018.
- (51) Iyer, R.; Tomar, S. K.; Uma Maheswari, T.; Singh, R. *Streptococcus thermophilus* strains: Multifunctional lactic acid bacteria. *Int. Dairy J.* **2010**, *20*, 133–141.
- (52) Rôças, I. N.; Siqueira, J. F.; Santos, K. R. N. Association of *Enterococcus faecalis* With Different Forms of Periradicular Diseases. *J. Endod.* **2004**, *30*, 315–320.
- (53) Novikova, M.; Metlitskaya, A.; Datsenko, K.; Kazakov, T.; Kazakov, A.; Wanner, B.; Severinov, K. The *Escherichia coli* Yej transporter is required for the uptake of translation inhibitor microcin C. *J. Bacteriol.* **2007**, *189*, 8361–8365.
- (54) Jumper, J.; Evans, R.; Pritzel, A.; Green, T.; Figurnov, M.; Ronneberger, O.; Tunyasuvunakool, K.; Bates, R.; Židek, A.; Potapenko, A.; Bridgland, A.; Meyer, C.; Kohl, S. A. A.; Ballard, A. J.; Cowie, A.; Romera-Paredes, B.; Nikolov, S.; Jain, R.; Adler, J.; Back, T.; Petersen, S.; Reiman, D.; Clancy, E.; Zielinski, M.; Steinegger, M.; Pacholska, M.; Berghammer, T.; Bodenstein, S.; Silver, D.; Vinyals, O.; Senior, A. W.; Kavukcuoglu, K.; Kohli, P.; Hassabis, D. Highly accurate protein structure prediction with AlphaFold. *Nature* **2021**, *596*, 583–589.
- (55) Mirdita, M.; Schütze, K.; Moriawaki, Y.; Heo, L.; Ovchinnikov, S.; Steinegger, M. ColabFold - Making protein folding accessible to all *bioRxiv* **2021**, DOI: 10.1101/2021.08.15.456425.
- (56) Dong, S.-H.; Kulikovskiy, A.; Zukher, I.; Estrada, P.; Dubiley, S.; Severinov, K.; Nair, S. K. Biosynthesis of the RiPP trojan horse nucleotide antibiotic microcin C is directed by the N-formyl of the peptide precursor. *Chem. Sci.* **2019**, *10*, 2391–2395.
- (57) Saitou, N.; Nei, M. The neighbor-joining method: a new method for reconstructing phylogenetic trees. *Mol. Biol. Evol.* **1987**, *4*, 406–425.
- (58) Le, K. Y.; Otto, M. Quorum-sensing regulation in *staphylococci*—an overview. *Front. Microbiol.* **2015**, *6* (6), No. 1174.
- (59) Du, L.; Lou, L. PKS and NRPS release mechanisms. *Nat. Prod. Rep.* **2010**, *27*, 255–278.
- (60) Walsh, C. T. Polyketide and nonribosomal peptide antibiotics: modularity and versatility. *Science* **2004**, *303*, 1805–1810.
- (61) Staunton, J.; Weissman, K. J. Polyketide biosynthesis: a millennium review. *Nat. Prod. Rep.* **2001**, *18*, 380–416.
- (62) Harvey, A. L. Natural products in drug discovery. *Drug Discovery Today* **2008**, *13*, 894–901.
- (63) Maksimov, M. O.; Pan, S. J.; Link, A. J. Lasso peptides: structure, function, biosynthesis, and engineering. *Nat. Prod. Rep.* **2012**, *29*, 996–1006.
- (64) Hegemann, J. D.; Zimmermann, M.; Xie, X.; Marahiel, M. A. Lasso peptides: an intriguing class of bacterial natural products. *Acc. Chem. Res.* **2015**, *48*, 1909–1919.
- (65) Miller, M. B.; Bassler, B. L. Quorum Sensing in Bacteria. *Annu. Rev. Microbiol.* **2001**, *55*, 165–199.
- (66) Novick, R. P.; Geisinger, E. Quorum Sensing in Staphylococci. *Annu. Rev. Genet.* **2008**, *42*, 541–564.